Distances between Active Site Probes in Glutamine Synthetase from *Escherichia coli*: Fluorescence Energy Transfer in Free and in Stacked Dodecamers

Michael R. Maurizi, Philip G. Kasprzyk, and Ann Ginsburg*

Laboratory of Molecular Biology, National Cancer Institute, and Section on Protein Chemistry, Laboratory of Biochemistry, National Heart, Lung, and Blood Institute, National Institutes of Health, Bethesda, Maryland 20892

Received May 30, 1985

ABSTRACT: Probes for fluorescence energy transfer measurements were introduced into active sites of dodecameric glutamine synthetase from *Escherichia coli* by substituting appropriate ATP analogues for ATP in the autoinactivation reaction of this enzyme with L-Met-(*S*)-sulfoximine and Mn^{2+} [Maurizi, M. R., & Ginsburg, A. (1986) *Biochemistry* (preceding paper in this issue)]. Two fluorescent donors, 8-mercapto-ATP alkylated with either 5-[[[(iodoacetyl)amino]ethyl]amino]naphthalene-1-sulfonic acid (AEDANS-ATP) or 1,N^6-etheno-2-aza-ATP (aza-ε-ATP), and two acceptors, 6-mercaptopurine ribonucleotide triphosphate or 8-mercapto-ATP alkylated with the chromophore 4′-[[4-(dimethylamino)-phenyl]azo]-2-iodoacetanilide (6-Y- or 8-Y-ATP), were used. Fluorescence emissions of enzyme derivatives with 1 or 2 equiv of fluorescent donor per dodecamer and either an acceptor (Y) or ADP at the remaining active sites were compared at pH 7.0. The results, together with the known geometry of the enzyme, indicate that active site probes in the dodecamer are widely separated and that energy transfer occurs from a single donor to two or three acceptors on adjacent subunits. The calculated distance between equidistant active site probes on heterologously bonded subunits within the same hexagonal ring is 56–60 Å. Probes on isologously bonded subunits are no closer than 60 Å and may be as far apart as 78 Å. Thus, active sites are away from the 6-fold axis of symmetry toward the outer edges of the dodecamer and are located ≥30 Å from the plane separating the hexagonal rings. During Zn^{2+}-induced stacking of the same enzyme derivatives along the 6-fold axes of symmetry, additional quenches of fluorescent probes were dependent on the presence of acceptors on separate dodecamers. The Zn^{2+}-induced face to face aggregation of dodecamers in the presence of 46 μM $ZnCl_2$ and 9 mM $MgCl_2$ at pH 7.0 had an Arrhenius activation energy of 22.3 ± 0.2 kcal/mol and a second-order rate constant at 25 °C of $\sim 10^5$ M^{-1} s^{-1} at early stages. Time-dependent fluorescence quenches correlated well with the degree of linear polymer formation and reached maximum values of 47–70% quench when the average *n*-mer was six dodecamers. After correction for unquenched polymer ends, a fluorescent donor and an acceptor probe in layered dodecamers were estimated to be ~36 Å apart—an average value if there is some twisting of single strands. This intermolecular energy-transfer distance confirms that active site nucleotide probes are toward exterior surfaces away from the lateral plane separating hexagonal rings of a dodecamer.

Electron micrographs of negatively stained glutamine synthetase from *Escherichia coli* together with physical-chemical information (Shapiro & Ginsburg, 1968) allowed Valentine et al. (1968) to propose a molecular structure for this enzyme that has remained essentially correct as improved electron microscopic techniques have evolved. Glutamine synthetase is composed of 12 identical subunits (of M_r 50 000 each) that are structurally arranged in two superimposed hexagonal rings of ~140 Å in diameter. Because the native manganese enzyme normally exists as a closed dodecameric structure, Valentine et al. (1968) proposed a 6-fold dihedral symmetry for the glutamine synthetase molecule with subunits within a ring heterologously bonded and subunits from opposing rings in isologous contacts. Centers of subunits from either ring are ~45 Å apart. Later, it was found that all subunits of the enzyme express activity (Hunt et al., 1975) and that the active site of each subunit has binding sites for two M^{2+}, nucleotide, and L-glutamine or L-glutamate (Hunt et al., 1975; Shrake et al., 1977) or 2 M^{2+}, L-Met-(*S*)-sulfoximine phosphate, and ADP in the case of a transition-state complex (Maurizi& Ginsburg, 1982a). From various estimates, intrasubunit active site dimensions (including the adenylylation site) can be approximated by a sphere of ~12 Å diameter (Villafranca et al., 1978).

Changes in subunit interactions in glutamine synthetase are produced by binding ligands to active sites and by adenylylation of subunits. The conformational change that occurs when Mn^{2+} (or Mg^{2+}) binds to high-affinity (n_1) sites of the apoenzyme is slower when subsaturating amounts of M^{2+} are added (Hunt & Ginsburg, 1972). When the enzyme is inactivated to increasing extent by the binding of the transition-state complex, the residual active sites undergo an increasingly slower conformational change when EDTA is added to remove Mn^{2+} (Maurizi & Ginsburg, 1986). In addition, negative cooperativity (due presumably to homologous subunit interactions) in binding substrates and the L-glutamate analogue L-Met-(*S*)-sulfoximine (Meister, 1974) has been observed (Denton & Ginsburg, 1970; Bild & Boyer, 1980; Rhee et al., 1981; Shrake et al., 1982; Wedler et al., 1982). Furthermore, autoinactivation of glutamine synthetase by phosphorylation of L-Met-(*S*)-sulfoximine in the presence of ATP and Mn^{2+} enormously strengthens intersubunit bonding domains (Maurizi & Ginsberg, 1982b). Heterologous subunit interactions are suggested by the fact that adenylylation, which inactivates Mg^{2+}-supported biosynthetic activity of adenylylated subunits, alters K_m values for L-glutamate in this reaction catalyzed by active subunits (Stadtman & Ginsburg, 1974).

* Address correspondence to this author at the National Heart, Lung, and Blood Institute, Building 3, Room 208, Bethesda, MD 20892.

How do events occurring at active sites of glutamine synthetase influence subunit interactions? We already know that the binding of active site ligands introduces some asymmetry into the dodecameric enzyme and that dissociation of the partially liganded enzyme occurs by a preferential breaking of heterologous intraring contacts between subunits while leaving isologous subunit contacts intact (Maurizi & Ginsburg, 1982b; Haschemeyer et al., 1982). Also, under certain conditions, glutamine synthetase dodecamers are deformed by divalent cations (e.g., Co^{2+}, Zn^{2+}, or Mn^{2+}) in such a way so as to produce spontaneous face to face aggregation along the 6-fold axes of dodecamers, which eventually leads to side to side interactions between stacked dodecamers and paracrystalline bundles (Valentine et al., 1968; Miller et al., 1974; Frey et al., 1975; Lipka et al., 1984; Frey & Eisenberg, 1984). Locating the active site on each subunit and determining the distances between active sites in the dodecameric enzyme are essential steps toward understanding how active site ligands promote subunit interactions.

The accompanying paper (Maurizi & Ginsburg, 1986) describes the procedures for labeling active sites of glutamine synthetase that were used in this paper to introduce specific probes for energy-transfer measurements. Our results together with the known geometry of the enzyme indicate that active site probes in the dodecamer are widely separated.

Materials and Methods

Unadenylylated glutamine synthetase was isolated and stored as described in the accompanying paper (Maurizi & Ginsburg, 1986). IAEDANS[1] and 4′[[4-(dimethylamino)-phenyl]azo]-2-iodoacetanilide (acceptor Y) were purchased from Molecular Probes, and aza-ε-ATP was a gift from Dr. Sue Goo Rhee in our laboratory. Quinine sulfate was obtained from Aldrich Chemical Co., and ATP, L-Met-(*RS*)-sulfoximine, and Hepes were from Sigma Chemical Co. Water was distilled and then deionized and filtered through a Millipore Milli-Q2 reagent-grade system. A stock solution of $ZnCl_2$ was prepared from 99.9% pure mossy Zn in 10% excess 6 N HCl (final pH $\simeq$2). Chelex 100 (100–200 mesh) and Bio-Gel P-10 (200–400 mesh) were from Bio-Rad. Hepes/KOH (40 mM) buffer at pH 7.0 was freed of metal ions by passage through a 5 × 3.3 cm column of Chelex 100 in the K^+ form and degassed before use (Hunt & Ginsburg, 1980). All other chemicals were analytical reagent-grade.

Preparation of 6-Y-ATP and 8-Y-ATP. After 5 mg of 6-mercaptopurine ribonucleoside triphosphate or of 8-mercapto-ATP (Maurizi & Ginsburg, 1986) was dissolved in 50 μL of water, 450 μL of 0.1 M triethanolamine in 75% dimethylformamide, pH 9.7, was added. Then, 10 mg of 4′-[[4-dimethylamino)phenyl]-2-iodoacetanilide (iodo-Y) was added, and the reaction mixture was covered with aluminum foil and left at room temperature for 4 h. The mercapto-ATP derivatives reacted quantitatively in this time. Water was added, and the precipitate (unreacted iodo-Y) was discarded after centrifugation. A small amount of 1 M LiCl and then 9 volumes of ethanol were added to precipitate the nucleotide analogue in the supernatant. This mixture was stored at −20 °C overnight. The Y-ATP was crystallized 3 times from 90% EtOH at −20 °C. The purity of Y-ATP was determined by thin-layer chromatography on cellulose with isobutyric acid/concentrated NH_4OH/H_2O (66/1/33), which confirmed the absence of unreacted mercaptonucleotides (<2%). The absence of unreacted mercapto nucleotides was also evident from the absorption spectra of the products, which showed the large blue-shift characteristic of alkylation of the mercapto nucleotides (Maurizi & Ginsburg, 1986). The spectrum of the chromophore, iodo-Y, also is slightly blue-shifted upon reaction with 6-S-ATP, and the lithium salts of 6-Y-ATP and 8-Y-ATP are easily distinguished by color—dark yellow for 6-Y-ATP and bright red for 8-Y-ATP.

The extinction coefficient of the Y acceptor was determined to be 22 000 M^{-1} cm^{-1} at 465 nm by dissolving 4′-[[4-(dimethylamino)phenyl]azo]-2-iodoacetanilide, pH 7, in ~0.1 M glutathione and determining its spectrum. This value agrees with that reported by Luedtke et al. (1981).

Preparation and Characterization of Glutamine Synthetase Derivatives for Energy-Transfer Measurements. Partially inactive fluorescent enzyme derivatives (7.5 mg/incubation) were prepared by adding ~1 or ~2 equiv/dodecamer of either 8-S-AEDANS-ATP (Maurizi & Ginsburg, 1986) or aza-ε-ADP (stored at −20 °C as suspensions in ~33% ethanol) to the enzyme in a mixture of ~40 mM Hepes/KOH (pH 7.0), 1.0 mM $MnCl_2$, and 2.0 mM L-Met-(*RS*)-sulfoximine (final volume 1.5 mL). Reactions were incubated in the dark 20–60 min at room temperature and then at 4 °C overnight. Control incubations contained the enzyme and L-Met-(*RS*)-sulfoximine but no ATP analogue. Enzyme activity of aliquots removed during incubation was assayed by the pH 7.57 γ-glutamyl transfer method (Stadtman et al., 1979). Final percent activities of fluorescent enzyme derivatives were 91 and 82%, indicating that an average of ~1 and ~2 equiv of each fluorescent probe per dodecamer had been introduced, respectively. The four samples containing the fluorescent enzyme derivatives were each divided into three equal parts: 1 mM ATP was added to one-third, and ~100 μM of either 6-Y-ATP or 8-Y-ATP (see above) was added to another one-third. Samples again were incubated in the dark at 4 °C overnight and assayed for activity loss. If necessary, more 6-Y-ATP or 8-Y-ATP analogue was added, and samples were left at 4 °C for another 24 h. Final activity loss in each sample was >99%. Each of the 12 enzyme derivatives (~0.5 mL containing ~2.5 mg of protein) was gel-filtered through separate 10-mL Econo columns (Bio-Rad), which had been packed with Bio-Gel P-10 in 40 mM Hepes/KOH, pH 7.0, buffer. The columns were set up in a black-curtained box to exclude light, and enzyme derivatives were eluted with Chelex-treated 40 mM Hepes/KOH, pH 7.0, buffer. The enzyme derivative was collected in one tube (~1.2 mL). Samples were stored at 4 °C and were protected from the light at all times. Protein concentrations were determined in duplicate, with the Bio-Rad assay as described in the accompanying paper (Maurizi & Ginsburg, 1986), and ranged between 1.8 and 2.2 mg/mL. Duplicate fluorescence emission spectra (with excitation at 340 nm) and UV absorbance spectra were recorded for 10-fold dilutions of all enzyme derivatives from the Bio-Gel P-10 columns. With excitation at 340 nm, emission maxima were 490 nm for all 8-S-AEDANS-ADP inactive complexes and 460 nm for all aza-ε-ADP inactive enzyme complexes after correction for a minor contribution from the buffer. Since fluorescence

[1] Abbreviations: GS, glutamine synthetase; Hepes, 4-(2-hydroxyethyl)-1-piperazineethanesulfonic acid; IAEDANS, 5-[[[(iodoacetyl)-amino]ethyl]amino]naphthalene-1-sulfonic acid; 8-S-AEDANS-ATP, 8-mercapto-ATP alkylated with IAEDANS; AEDANS-ADP·GS, GS inactivated with 8-S-AEDANS-ATP, L-Met-(*S*)-sulfoximine, and Mn^{2+}; aza-ε-ATP, 1,N^6-etheno-2-aza-ATP; aza-ε-ADP·GS, GS inactivated with aza-ε-ATP, L-Met-(*S*)-sulfoximine, and Mn^{2+}; 8-Y-ATP or 6-Y-ATP, 8-mercapto-ATP or 6-mercaptopurine ribonucleoside triphosphate, respectively, alkylated with the Y (yellow) acceptor 4′-[[4-(dimethylamino)phenyl]azo]-2-iodoacetanilide; 8-Y-ADP·GS or 6-Y-ADP·GS, GS inactivated with 8-Y-ATP or 6-Y-ATP, respectively, in the presence of L-Met-(*S*)-sulfoximine and Mn^{2+}.

emission spectra were the same in the absence and presence of energy acceptors, the quantum yields of the donors were proportional to the fluorescence measured at emission maxima. By use of the wavelength of maximum emission (with excitation at 340 nm), the fluorescence intensity of each of the 12 enzyme derivatives also was determined in four to five separate measurements of different 40-fold dilutions into 40 mM Hepes/KOH, pH 7.0, buffer. Band-pass settings were kept constant with 4- and 6-nm slits used for excitation and emission, respectively. The percent transmission of diluted samples was determined at 340 nm in a spectrophotometer. Absorbance measurements of inactive enzyme derivatives containing 6-Y- or 8-Y-ADP indicated that available active sites had been saturated with either chromophore. A Perkin-Elmer Model 650/40 fluorometer and a Model 320 spectrophotometer (with samples thermostated at 25 °C) were used for these measurments.

Other Fluorescence Measurements. For fluorescence measurements, cuvettes were soaked overnight in 0.5% HCl and then overnight in diluted Micro cleaning solution (International Products, Corp.). Following this treatment, cells were soaked and then rinsed thoroughly with deionized water.[2]

Corrected fluorescence spectra were recorded on an Aminco-Bowman spectrofluorometer (Chen, 1967) in the laboratory of Dr. Raymond F. Chen (NHLBI, NIH). The method of Parker & Rees (1966) was used to determine the quantum yield, with quinine sulfate in 0.1 M H_2SO_4 as the standard, which was assumed to have an absolute quantum yield of 0.70 (Scott et al., 1970). The absorbance of samples was kept below 0.05 (1.0-cm light path) to minimize inner filter effects.

Steady-state polarizations were determined by the method of Azumi & McGlynn (1966) with excitation at 340 nm (4-nm slit) and emission either at 490 nm (6-nm slit) with AEDANS-ADP enzyme derivatives or 460 nm (6-nm slit) with aza-ε-ADP enzyme derivatives. Fluorescence polarization, P, was measured at 25 °C with a Perkin-Elmer 650/40 fluorometer equipped with polarization accessories (C. N. Wood Manufacturing Co.) using a correction factor for the photomultiplier sensitivity. The limiting polarization was determined by measuring polarizations for a series of solutions of enzyme derivatives in 0–50% sucrose (w/v) in Hepes buffer, pH 7.0 (corrected for readings obtained with buffer–sucrose alone), and extrapolating Perrin plots of P vs. T/η to $T/\eta = 0$, where T is the absolute temperature and η is the solvent viscosity.

Analysis of Fluorescence Data. Energy transfer is related to the distance (R) between the fluorescing and absorbing species (Förster, 1959) as set forth in eq 1, where E is the

$$R = R_0(E^{-1} - 1)^{1/6} \quad (1)$$

observed efficiency of energy transfer and R_0 is the distance for 50% energy transfer. The quantity R_0 may be calculated from the known properties of the donor and acceptor (Brand & Witholt, 1967; Stryer, 1978) according to

$$R_0 = (9.785 \times 10^3)(J\kappa^2 Q_D n^{-4})^{1/6} \quad (2)$$

where n is the refractive index of the protein solution (~1.4 for enzyme derivatives in Hepes buffer), Q_D is the quantum yield of the donor, κ^2 is an orientation factor dependent on the relative orientations of the donor and acceptor dipoles and was assumed to be $^2/_3$ for random orientation (as discussed below), and J is the normalized spectral overlap integral between fluorescent donor and absorbing acceptor (see Figure 1). The spectral overlap integral is a measure of how well the fluorescence emission of the donor overlaps the absorbance of the acceptor and is given by the equation (Stryer, 1978)

$$J = \int F(\lambda)\epsilon(\lambda)\lambda^4 \, d\lambda / \int F(\lambda) \, d\lambda \quad (3)$$

where $F(\lambda)$ is the donor fluorescence at wavelength λ (in cm) and $\epsilon(\lambda)$ is the molar extinction coefficient (in cm^{-1} M^{-1}) of the energy acceptor. The overlap integral was determined by graphical integration of the spectra. The fluorescence spectrum was summed over 1-nm intervals, and fractional fluorescence was multiplied by the absorption coefficient at each wavelength. Several alternate methods of integration (e.g., using 10-nm intervals) gave essentially the same results.

For intramolecular distance calculations, the efficiency of energy transfer was measured by comparing the fluorescence intensities of enzymes containing both donors and acceptors to comparable enzyme derivatives containing just the fluorescent donor with ADP at all other active sites of the dodecamer.[3] Fluorescence measurements of enzyme derivatives were made at two different protein concentrations (50 or 200 μg/mL ± 20%), and fluorescent values were normalized to the same protein concentration for the different enzyme derivatives. The percent transmittance of samples at the exciting wavelength (340 nm) was used to correct for inner filter effects in fluorescence measurements, using an effective pathway of 0.5 cm in a 1.0-cm cuvette for the latter corrections (≤6%).

The efficiency of energy transfer was calculated from eq 4, where F_{DA} and F_D are the fluorescence intensities of the

$$E = 1 - F_{DA}/F_D \quad (4)$$

donor in the presence and absence of an acceptor, respectively. Since the presence of an acceptor did not alter the shape of the donor emission spectrum, the quantum yield was proportional to the fluorescence at a given wavelength. In calculations of transfer to equidistant acceptors, it was assumed that each acceptor contributed equally to the quenching of the donor emission. If the probability of unquenched emission in the presence of a single acceptor is p, then the probability of unquenched emission in the presence of two equidistant acceptors is p^2. For a single acceptor, $p = F_{DA}/F_D$; for two equidistant acceptors, $p^2 = F_{DA}/F_D$ or $p = (F_{DA}/F_D)^{1/2}$, and the efficiency of transfer to each site $E = 1 - (F_{DA}/F_D)^{1/2}$; similarly, transfer efficiency to each site when there are three equidistant acceptors is calculated from $E = 1 - (F_{DA}/F_D)^{1/3}$.

For intermolecular distance calculations, the efficiency of energy transfer was estimated from the observed plateau value in fluorescence quench after $ZnCl_2$ had been added to produce face to face aggregation (see Results). Corrections for unquenched ends of linear polymers were based on the average number of dodecamers in stacks at the time of the maximum fluorescence quench.

[2] It was extremely important in these studies to avoid metal ion contaminants. For example, if fluorescence cuvettes were rinsed with H_2SO_4–chromate cleaning solution and then soaked for days with deionized water (with water changes), the observed rate of Zn^{2+}-induced aggregation of dodecamers still could be enhanced over that observed in cells cleaned without acid–chromate treatment.

[3] It should be noted that our measurements of energy transfer were with probes attached to nucleotide analogues bound to enzyme active sites. We have not attempted to correct our distance estimates for either the size of the probe or the point of attachment of the probe to the nucleotide analogue. When fully extended, the centers of AEDANS and Y structures are 7–9 Å from the center of the purine ring. However, the conformations of these nucleotide analogues at enzyme active sites are unknown. The agreement in distance measurements with 8-S-AEDANS-ADP and aza-ε-ADP (which is essentially the same size as ADP) suggests that the average position of the AEDANS group is close to that of aza-ε-ADP.

Table I: Fluorescence Properties of the Donor ATP Analogues[a]

	8-S-AEDANS-ATP free in solution	8-S-AEDANS-ATP bound to GS	aza-ε-ATP free in solution	aza-ε-ATP bound to GS
excitation (max) (nm)	340	340	340	340
emission (max) (nm)	490	490	490	460
quantum yield	0.27[b]	0.50 ± 0.05[c]	0.20 ± 0.04	0.48 ± 0.05
polarization	0.02 ± 0.01	0.28 ± 0.02	0.03 ± 0.01	0.24 ± 0.02
limiting polarization		0.35 ± 0.02		0.31 ± 0.02

[a] Measurements were made at 25 °C in chelex-treated 40 mM Hepes/KOH, pH 7.0, or 20 mM Hepes/KOH–100 mM KCl, pH 7.1, buffer. [b] Value in agreement with that of Hudson & Weber (1973). [c] Calculated from the quantum yield of free 8-S-AEDANS-ATP and the measured fluorescence enhancement on binding to active sites of the enzyme.

Electron Microscopy (STEM) Imaging. Scanning transmission electron microscopy (STEM) was performed at the Brookhaven National Laboratory. Dr. James J. Lipka and George Latham helped with biochemical preparations for STEM operation and Kristin D. Elmore prepared the grids and electron micrographs. Computer analysis and mass measurements were performed by J. J. Lipka as previously described (Lipka et al., 1984).

The preparation of carbon films, specimen application, freeze-drying, and STEM imaging were as described by Mosesson et al. (1981). The inactive enzyme complex with ADP, Mn^{2+}, and L-Met-(*S*)-sulfoximine phosphate at all active sites was in 20 mM Hepes/KOH–100 mM KCl (pH 7.1) at either 30 μg/mL without Zn^{2+} or at 100 μg/mL with 50 μM $ZnCl_2$ and 10 mM $MgCl_2$ present. Tobacco mosaic virus (as an internal calibration standard for mass measurements) in deionized water was applied first to carbon films, and then the glutamine synthetase solution (2.5 μL) was applied to the grid with the same volume of buffer. After 15–30 s was allowed for attachment to the film, the grid was washed 4 times with 10 mM ammonium acetate (pH 7.0) at 15-s intervals (Mosesson et al., 1981). During Zn^{2+}-induced aggregation of the inactive enzyme, samples were applied to carbon films at 4, 10.5, and 30 min after Zn^{2+} addition. STEM scans were collected at 512 × 512 nm (10-Å pixels) or at 1024 × 1024 nm (20-Å pixels). Photographs of STEM electron micrographs were taken by Dr. J. J. Lipka and Frank Kito.

Results

Intramolecular Fluorescence Energy Transfer between Active Site Probes. Two fluorescent donors were used in these studies: one was obtained by alkylation of 8-mercapto-ATP with IAEDANS (Hudson & Weber, 1973), and the other was aza-ε-ATP (Yip & Tsou, 1973). Either fluorescent donor could be introduced into 1–12 active sites of glutamine synthetase by phosphorylation of L-Met-(*S*)-sulfoximine in the presence of Mn^{2+}. Table I summarizes fluorescent properties of these ATP analogues when free or bound to active sites of the enzyme. Fluorescence intensities of 8-S-AEDANS-ATP and aza-ε-ATP were directly proportional to the extent of binding to active sites, indicating that the fluorescence properties of either bound probe were independent of ligand binding to adjacent subunits. The emission spectra (with excitation = 340 nm) of 8-S-AEDANS ATP and aza-ε-ATP were altered in different ways upon binding to the enzyme. The emission spectrum was slightly blue-shifted (1–2 nm) on binding 8-S-AEDANS-ATP to active sites, and the fluorescence increased nearly 2-fold. For aza-ε-ATP, the emission maximum was blue-shifted ~30 nm upon binding to the enzyme and the fluorescence increased ~2.4-fold. The fluorescence polarization of both probes also increased upon binding to the enzyme, indicating that the mobilities of the nucleotide probes were less than when free to rotate in solution. Corrected emission spectra with 340-nm excitation for enzyme-bound 8-S-AEDANS-ADP and aza-ε-ADP are shown in Figure 1.

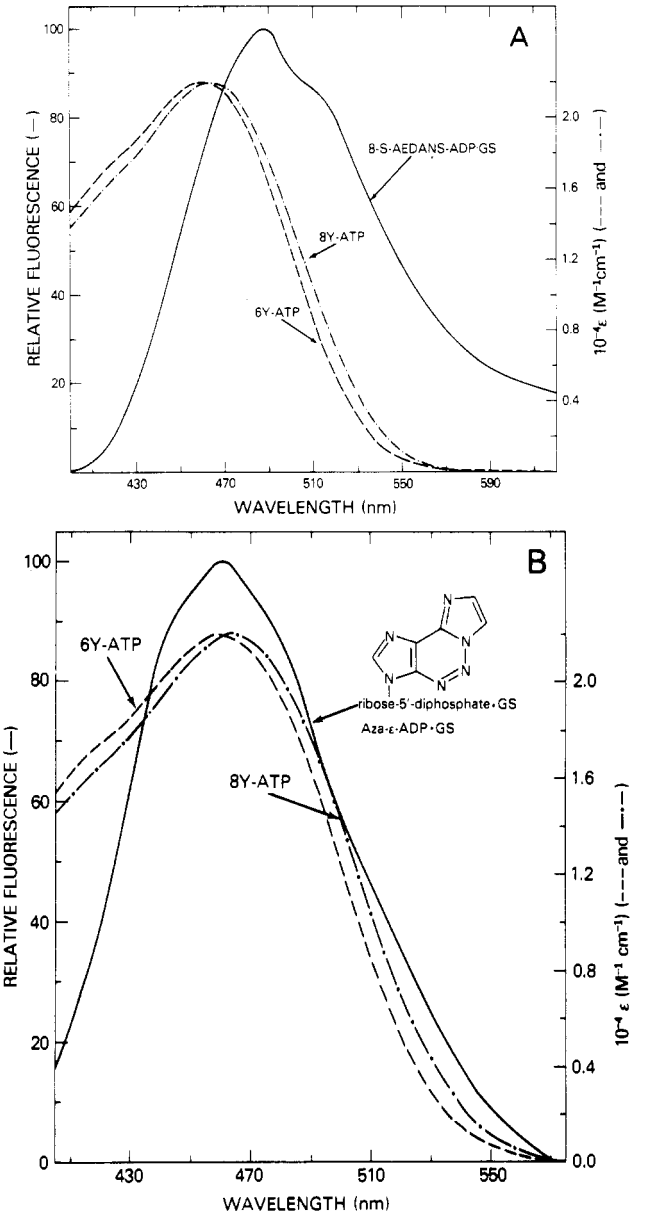

FIGURE 1: Spectral overlaps of corrected fluorescence emission spectra (340-nm excitation) of enzyme-bound 8-S-AEDANS-ADP [solid line in (A)] and aza-ε-ADP [solid line in (B)] with molar absorbance spectra of 8-Y-ATP (– · –) and 6-Y-ATP (– –). The calculated overlap integrals, *J*, for the four combinations 8-S-AEDANS-ADP·GS/8-Y-ATP, 8-S-AEDANS-ADP·GS/6-Y-ATP, aza-ε-ADP·GS/8-Y-ATP, and aza-ε-ADP·GS/6-Y-ATP are 6.61×10^{-14}, 5.82×10^{-14}, 8.08×10^{-14}, and 7.80×10^{-14} M^{-1} cm^3, respectively. Measurements were performed at 25 °C in 40 mM Hepes/KOH, pH 7.0, buffer.

The chromogen 4′-[[4-(dimethylamino)phenyl]azo]-2-iodoacetanilide was used to alkylate 8-mercapto-ATP and 6-mercaptopurine ribonucleoside triphosphate to produce 8-Y-ATP and 6-Y-ATP, respectively. These nucleotide ana-

Table II: Intramolecular Distances between Active Site Probes on Glutamine Synthetase

donor/acceptor on enzyme active sites	R_0 (Å)[a]	% transfer efficiency[b]	R (Å) (one acceptor)[c]	R (Å) (two acceptors)[c]	R (Å) (three acceptors)[c]
8-S-AEDANS-ADP/6-Y-ADP	41	25 ± 4 (8)	49 ± 2	56 ± 2	60 ± 2
8-S-AEDANS-ADP/8-Y-ADP	41	22 ± 4 (10)	51 ± 2	57 ± 2	62 ± 2
aza-ε-ADP/6-Y-ADP	42	32 ± 2 (6)	48 ± 1	54 ± 1	58 ± 1
aza-ε-ADP/8-Y-ADP	43	37 ± 4 (6)	47 ± 1	54 ± 1	58 ± 1

[a] R_0 is the calculated critical transfer distance (see text) for an efficiency of energy transfer of 50%. [b] The number of independent determinations of fluorescence quench for each donor/acceptor pair, as measured by simultaneous comparison to the control (fluorescent donor/ADP pair; see text), is given in parentheses and the standard deviation from the average value is indicated. [c] R is the distance between active site probes of glutamine synthetase calculated according to eq 1. The transfer efficiencies for each donor/acceptor pair for one, two, and three equidistant acceptors were determined from the appropriate form of eq 4 (see Materials and Methods). Error estimates were made by calculating R from $E \pm$ SD.

logues were chosen as acceptors since the Y chromophore is highly absorbant at ~465 nm ($\epsilon \approx 22\,000$ M^{-1} cm^{-1}) and the absorbance spectrum overlaps well with the fluorescence emission spectra of 8-S-AEDANS-ATP and aza-ε-ATP. The overlaps of the spectra of 8-Y-ATP and 6-Y-ATP with fluorescence emission spectra of enzyme-bound 8-S-AEDANS-ADP and aza-ε-ADP are shown in panels A and B of Figure 1, respectively. The J values for integral overlaps are given in the legend to Figure 1.

Enzyme samples for fluorescence energy transfer distance measurements were prepared by introducing ATP analogues into active sites of glutamine synthetase by phosphorylation of L-Met-(*S*)-sulfoximine in the presence of Mn^{2+} at pH 7.0. The extent of incorporation of any probe could be followed conveniently by activity loss. Enzyme derivatives also could be easily freed of unbound or loosely bound ligands by dialysis or gel filtration, since the binding of the inactivating active site ligands is essentially irreversible at pH 7 (Maurizi & Ginsburg, 1986). The enzyme samples contained an average of 1 or 2 equiv of fluorescent donor complexed to active sites per dodecamer with the remaining 11 or 10 active sites per molecule occupied by the acceptors, 6-Y-ADP or 8-Y-ADP, or by ADP as the control. The fluorescence of enzyme with 1 or 2 equiv of fluorescent donor per dodecamer was unchanged if the remaining subunits had ADP bound at the active sites. However, when 6-Y-ATP or 8-Y-ATP was bound to the remaining active sites, a substantial quenching of the fluorescence was seen (Maurizi & Ginsburg, 1986). The percent quench was calculated in each case by reference to an equivalent concentration of unquenched enzyme derivative (control) containing 1 or 2 equiv of the fluorescent donor per dodecamer and ADP at remaining active sites.

The design of the experiments of this paper was based on results presented in the accompanying paper of Maurizi & Ginsburg (1986), which showed that quenching of the fluorescence of 8-S-AEDANS-ADP bound to active sites of glutamine synthetase was dependent upon binding the 6-mercaptopurine ribonucleoside triphosphate analogue bearing the Y chromophore to other active sites within the dodecamer and was attributable to energy transfer from the fluorescent donor to this acceptor. Three types of evidence indicated that the 6-Y-ATP analogue binds to active sites of the enzyme: (1) Blocking active sites by phosphorylation of L-Met-(*S*)-sulfoximine with ATP prevented the binding of 6Y-ATP to glutamine synthetase. (2) Reversibly bound 6-Y-ATP was displaced by excess ATP. (3) The addition of L-Met-(*S*)-sulfoximine with 6-Y-ATP inactivated the enzyme in an analogous reaction to the autoinactivation reaction observed with L-Met-(*S*)-sulfoximine and ATP (Maurizi & Ginsburg, 1982a).

We conclude that the observed quench produced by the binding of Y-ADP analogues at nearby active sites in Table II is due to fluorescence energy transfer, and we have used the percentage quench to calculate the transfer efficiency according to eq 4. In four to five separate measurements at the two protein concentrations, the percent transfer efficiency was the same for each donor/acceptor pair whether 1 or 2 equiv of fluorescent donor/dodecamer was bound. Accordingly, 6–10 separate measurements on samples containing 1 or 2 equiv of donor/dodecamer for each donor/acceptor pair were averaged (Table II).

Values of R_0 for donor/acceptor pairs in Table II were calculated from the measured quantum yields of protein-bound donors (Table I), the overlap integrals (Figure 1), and an assumed orientation factor of $^2/_3$ (see below), according to eq 2. Values of R in Table II were calculated from eq 4 and 1 and had a precision ±2 Å; there was good agreement between these values for the four donor/acceptor pairs.

Values of R were calculated in Table II for one, two, or three equidistant acceptors. These three cases reflect different possible simplifying assumptions, which will be addressed in more detail under Discussion. The *one acceptor case* would apply to transfer from a donor to an acceptor on an isologously bonded subunit from the opposite hexameric ring. Because of the 6th power dependence of the transfer efficiency on R, this case would apply only if the distances between these pairs of active sites were much shorter than the distances between these sites and the active sites of subunits within the same ring. The *two acceptor case* refers to energy transfer between probes attached to active sites of subunits heterologously bonded within a hexagonal ring. The subunit containing the fluorescent donor would be flanked by subunits containing the bound acceptor, and energy transfer could occur to equidistant acceptor probes at two adjacent active sites. In the latter case, probes at active sites of isologously bonded subunits are farther apart than those within the same ring. In the *three acceptor case*, probes at active sites on the three subunits adjacent to the subunit containing the fluorescent donor are approximately equidistant, which would be true if active site probes of isologously bonded subunits are about the same distance apart as are probes on heterologously bonded subunits within the same hexagonal ring. The low efficiency of energy transfer observed in our measurements suggests that either the two or three acceptor case is correct.

Intermolecular Energy Transfer between Active Site Probes on Glutamine Synthetase in Stacked Dodecamers. The same fluorescent derivatives of the enzyme could be induced to form linear face to face polymers by Zn^{2+} addition in the presence of relatively high concentrations of Mg^{2+} at pH 7.0. There is one high-affinity Zn^{2+} binding site per subunit that is distinct from metal ion sites at the active site (Hunt et al., 1975). Miller et al. (1974) observed that Zn^{2+}-induced stacking of dodecameric glutamine synthetase is facilitated by saturating nonspecific divalent cation sites of the enzyme with Mg^{2+}, which produces no aggregation. The stacking reaction also can be readily reversed by the addition of EDTA to chelate the Zn^{2+} present.

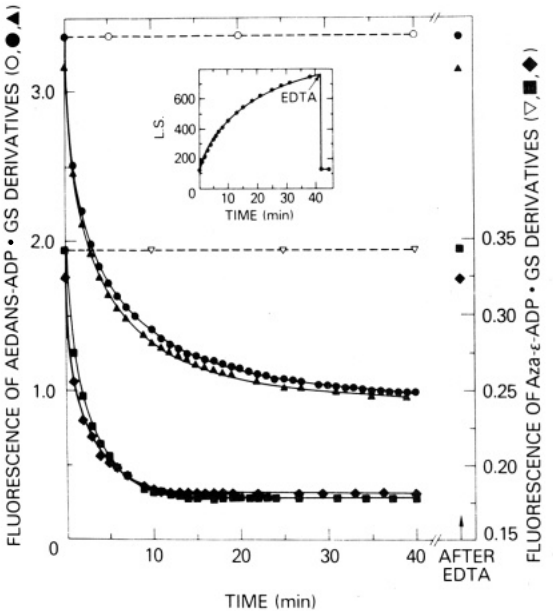

FIGURE 2: Time-dependent fluorescence and light scattering changes produced by Zn^{2+}-induced face to face stacking of fluorescent glutamine synthetase derivatives with probes bound at active sites. At zero time, 46 μM $ZnCl_2$ was added to enzyme derivatives (90–110 μg/mL) in a buffer composed of Chelex-treated 40 mM Hepes/KOH at pH 7.0 and 9.2 mM $MgCl_2$ thermostated at 25 °C in a Perkin-Elmer 650-40 fluorometer. Enzyme derivatives contained an average 1 equiv per dodecamer of the fluorescent active site probes 8-S-AEDANS-ADP (○, ●, ▲) or aza-ϵ-ADP (▽, ■, ♦) with the remaining 11 active sites blocked by the transition-state complex with ADP (open symbols) or with the acceptors of 6-Y-ADP (●, ■) or 8-Y-ADP (▲, ♦). For 8-S-AEDANS-ADP·GS and aza-ϵ-ADP·GS derivatives, fluorescence changes with 340-nm excitation were recorded at 490- or 460-nm emission, respectively. Light scattering changes (inset) were monitored with both excitation and emission wavelengths set at 360 nm. The inset shows the time course of 90° light scattering (LS) after Zn^{2+} addition to the 8-S-AEDANS-ADP/6-Y-ADP enzyme derivative (100 μg/mL); similar LS curves were obtained with the other derivatives used to obtain the data in this figure. The addition of 1.8 mM EDTA at 42–50 min reversed fluorescence and light scattering changes within the time of mixing (arrow).

Figure 2 shows fluorescence–time data at 25 °C after adding 46 μM $ZnCl_2$ at zero time to fluorescent derivatives of glutamine synthetase (~100 μg/mL) in the presence of 9 mM $MgCl_2$ at pH 7.0. When there was no acceptor bound to active sites, there was no change in fluorescence after adding Zn^{2+}, as shown by the open symbols in Figure 2 for the 8-S-AEDANS·GS/ADP and aza-ϵ-ADP·GS/ADP samples. When 6-Y-ADP or 8-Y-ADP acceptors were bound to ~11 active sites of the dodecamer containing about one fluorescent donor, the addition of Zn^{2+} produced a time-dependent fluorescence decrease. After 30–40 min, total quenches of ~70 and 55% were obtained for the enzyme derivatives containing 8-S-AEDANS-ADP and aza-ϵ-ADP, respectively. Note that the relative fluorescence of the aza-ϵ-ADP derivatives is one-tenth that of the 8-S-AEDANS-ADP enzyme derivatives.

During the time course of the fluorescence measurements, 90° light scattering values (Ex = Em = 360 nm) were obtained. A representative light scattering change as a function of time is shown in the inset to Figure 2. After 30 min there was an approximate 6-fold increase in light scattering; this value varied 5–8-fold in different experiments. At 30 min after Zn^{2+} addition, measured transmittance at 340 nm was 97–98% in a 1-cm light path. However, light scattering continued to increase after 30 min, after which time increases in turbidity could be measured. Presumably, side to side aggregation of linear polymers occurs at these later times as was earlier observed by Miller et al. (1974) for the native enzyme. Fluorescence changes appeared to plateau after 30–40 min (Figure 2), and it is reasonable to propose that the distribution of polymer ends was not significantly changing after 30–40 min.

The addition of 1.8 mM EDTA after ~40 min completely reversed the fluorescence and light scattering changes (Figure 2). Thus, the results in Figure 2 suggest that observed fluorescence decreases are coupled to the stacking reaction, which is reversed by chelation of Zn^{2+}.

The Zn^{2+}-induced face to face linear aggregation of inactive glutamine synthetase dodecamers was confirmed by STEM analysis. Figure 3 shows representative images of the manganese enzyme inactivated by L-Met-(*S*)-sulfoximine and ATP without Zn^{2+} (0 min) and at 4, 10.5, and 30 min after Zn^{2+} addition in the presence of 10 mM $MgCl_2$. The average number of dodecamers per linear polymer was 1.9 at 4 min, 2.9 at 10.5 min, and 5.8 at 30 min when 269, 276, and 180 particles, respectively, were measured in one to four different 1024 × 1024 nm STEM micrographs. At 30 min, ~45% of the particles consisted of six or more dodecamers. The bright

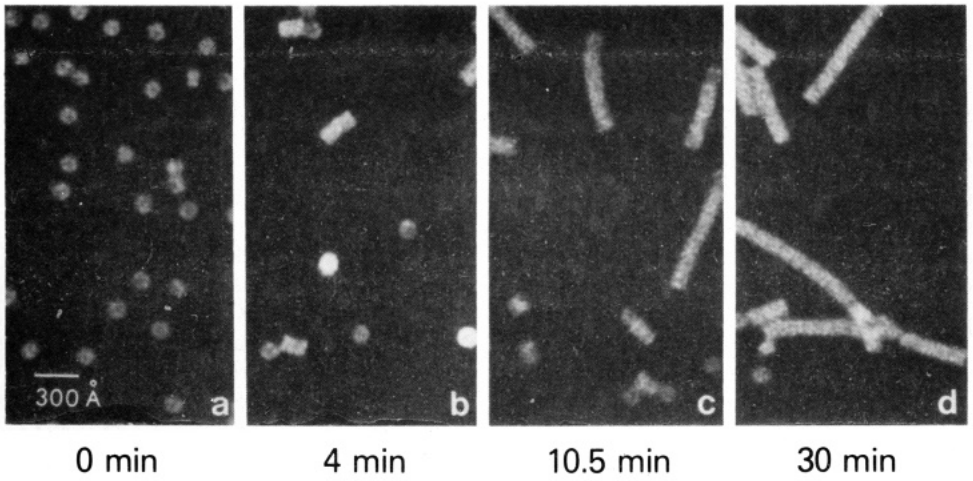

FIGURE 3: Representative STEM images of the inactive glutamine synthetase complex before (0 min) and after Zn^{2+} addition in the presence of 10 mM $MgCl_2$ at pH 7.0 (25 °C). For this analysis, glutamine synthetase was completely inactivated with L-Met-(*S*)-sulfoximine and ATP in the presence of 1 mM $MnCl_2$ and then dialyzed against 20 mM Hepes/KOH–100 mM KCl, pH 7.1, buffer. Panel a is a STEM micrograph prepared from the inactive enzyme at 30 μg/mL concentration. Panels b–d show representative fields from STEM images of samples removed at 4, 10.5, and 30 min after the addition of 50 μM $ZnCl_2$ to the inactive enzyme (100 μg/mL) at 25 °C in a buffer containing 20 mM Hepes, 100 mM KCl, and 10 mM $MgCl_2$ at pH 7.1. The field shown in each panel is ~18% of the recorded area in STEM 512 × 512 nm micrographs.

round images in panel b at 4 min are stacked dodecamers on end (i.e., coming out of the plane of the micrograph). Mass analysis of these bright images indicate that these can represent up to four stacked dodecamers (J. J. Lipka, personal communication). Also, many linear aggregates (especially apparent in panel c at 10.5 min) appear to have landed face down on the carbon film and subsequently during specimen preparation to have fallen sideways, resulting in the breaking off of one dodecameric unit (forming dotted i's) in the process. In our particle counting we did not count these obviously sheared off dodecamers as monomers.

Figure 4 shows the concentration dependence of fluorescence and light scattering changes as functions of time during Zn^{2+}-induced face to face aggregation of a glutamine synthetase derivative containing ~2 equiv of 8-S-AEDANS-ADP and ~10 equiv of the acceptor 8-Y-ADP at active sites. Portions of the data of Figure 4A are replotted in panel B to show the correlation between the increase in light scattering (expressed as the ratio of the value observed at each time to the initial value) as a function of the percent of the observed maximum quench in fluorescence. There is an excellent correlation between the percent of maximum fluorescence quench and the degree of polymerization at all four concentrations of the enzyme derivative. The data in Figure 4B extrapolate to a ratio of $[LS]_{obsd}/[LS]_{init}$ of ~6.5 at 100% of maximum fluorescence quench, which is in good agreement with the average *n*-mer of six dodecamers that was calculated from STEM images at 30 min (see above).

Figure 4C shows second-order rate plots of the fluorescence–time data at the four concentrations in Figure 4A for the Zn^{2+}-induced stacking reaction of the AEDANS-ADP/8-Y-ADP enzyme derivative. The linear portions of the plots in Figure 4C extrapolate to nearly the same values of $1/(F_0 - F_\infty)$ that were measured. Not unexpectedly, the data points of Figure 4C deviate from linearity at increasingly shorter times as the concentration of the dodecameric derivatives was increased. For second-order analysis, it was assumed that the quantity $F_t - F_\infty$ is proportional to unreacted dodecamer (monomer) and that F_∞ is the intrinsic fluorescence of stacked dodecamers present at the time of maximum quench. The average second-order rate constant of $(5 \pm 2) \times 10^4$ M^{-1} s^{-1} was in good agreement with the average second-order k value of $\sim 8 \times 10^4$ M^{-1} s^{-1} calculated from the data obtained in the first 4 min in Figure 2 with fluorescent enzyme derivatives containing ~1 equiv of either AEDANS-ADP or aza-ε-ADP per dodecamer. Since the intrinsic fluorescence of stacked dodecamers includes unquenched polymer ends, estimated second-order rate constants are ~3-fold greater than calculated from plots of $1/(F_t - F_\infty)$ vs. time.

Light scattering increases during the Zn^{2+}-induced stacking reaction also were measured as functions of temperature. Measurements were made as in the inset to Figure 2 from 15–40 °C at 5° intervals with 96 μg/mL of the inactive enzyme complex with ADP at active sites. Arrhenius plots of the log reciprocal of the doubling, tripling, and quadrupling time of the initial light scattering value vs. the reciprocal of the absolute temperature (K) were linear with correlation coefficients > 0.999. An Arrhenius activation energy of 22.3 ± 0.2 kcal/mol was obtained from these data for the face to face aggregation process.

Table III presents values for the maximum percent quench (percent transfer efficiency) obtained by Zn^{2+}-induced face to face aggregation of each donor/acceptor pair on active sites of dodecameric glutamine synthetase. Enzyme derivatives with an average of 1 or 2 equiv of the fluorescent donor are listed

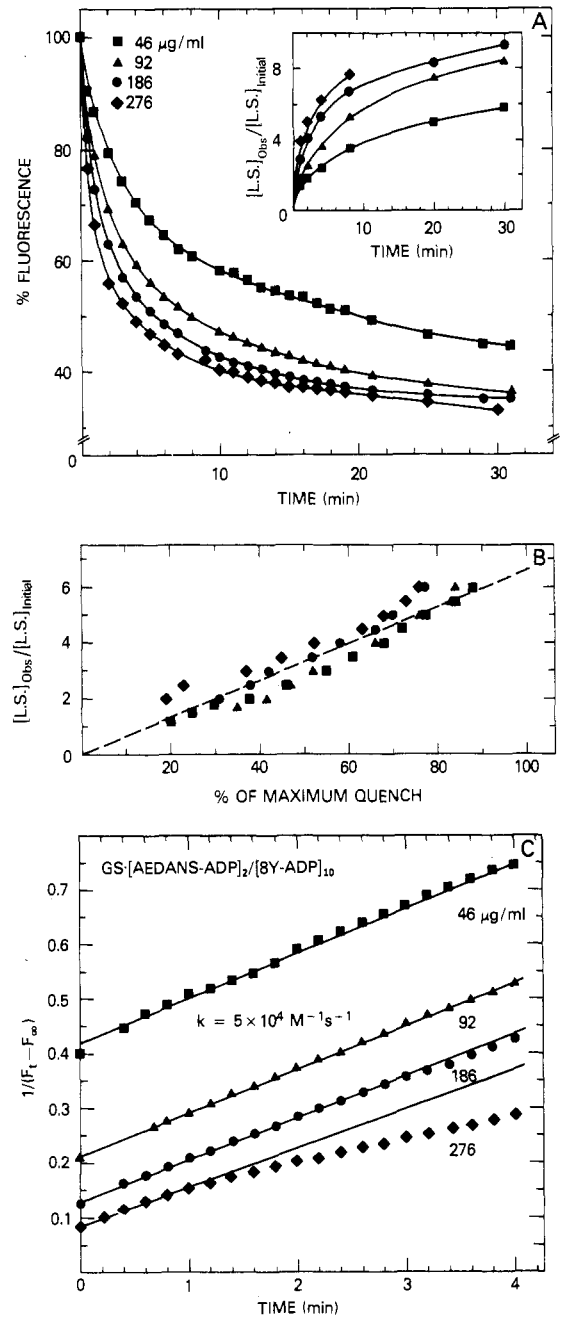

FIGURE 4: Concentration dependence of fluorescence and light scattering changes during Zn^{2+}-induced face to face aggregation of a glutamine synthetase derivative containing ~2 equiv/dodecamer of 8-S-AEDANS-ADP and ~10 equiv/dodecamer of the acceptor 8-Y-ADP at active sites. In (A), the fluorescence decay (Ex = 340 nm, Em = 490 nm) and light scattering increases (Ex = Em = 360 nm) were measured at 25 °C as functions of time after Zn^{2+} addition (46 μM) in the presence of 9.2 mM $MgCl_2$ at pH 7.0 (as described in the legend to Figure 2). The inset shows the ratio of the observed to initial light scattering (fold increase) vs. time for the four concentrations of the protein [46 (■), 92 (▲), 186 (●), and 276 μg/mL (♦)]. In (B), the ratio of observed to initial 90° light scattering values are plotted vs. the percent of maximum quench of fluorescence (using the 30-min value at 186 μg/mL and the same symbols). In (C), the initial changes in the fluorescence of (A) are plotted as second-order rate plots for self-association, assuming that the quantity $F_t - F_\infty$ is proportional to the concentration of the dodecameric enzyme (monomer) present at time t. Second-order rate constants [$k = (5 \pm 2) \times 10^4$ M^{-1} s^{-1}] were calculated from [slope × $(F_0 - F_\infty)$]/(60[M]), where [M] is the initial concentration of monomer (dodecamer). Initial (F_0) values of 3.88, 7.42, 12.63, and 17.95 and final (F_∞) values of 1.38, 2.64, 4.36, and 5.21 were measured for 46, 92, 186, and 276 μg/mL, respectively.

Table III: Intermolecular Distances between Active Site Probes in Stacked Glutamine Synthetase Dodecamers

donor/acceptor on enzyme active sites[a]	R_0 (Å)[b]	% maximum quench (transfer efficiency) obsd value[c]	% maximum quench (transfer efficiency) corr value[d]	R (Å)[e]
$[8\text{-S-AEDANS-ADP}]_1/-[6\text{-Y-ADP}]_{11}$	41	70*	78	33
$[8\text{-S-AEDANS-ADP}]_1/-[8\text{-Y-ADP}]_{11}$	41	69	77	34
$[\text{aza-}\epsilon\text{-ADP}]_1/-[6\text{-Y-ADP}]_{11}$	42	47*	55	41
$[\text{aza-}\epsilon\text{-ADP}]_1/-[8\text{-Y-ADP}]_{11}$	43	47*	55	42
$[8\text{-S-AEDANS-ADP}]_2/-[6\text{-Y-ADP}]_{10}$	41	61	78	33
$[8\text{-S-AEDANS-ADP}]_2/-[8\text{-Y-ADP}]_{10}$	41	63*	80	33
$[\text{aza-}\epsilon\text{-ADP}]_2/-[6\text{-Y-ADP}]_{10}$	42	56	73	36
$[\text{aza-}\epsilon\text{-ADP}]_2/-[8\text{-Y-ADP}]_{10}$	43	54	71	37

[a] The subscripts refer to the average number per dodecamer of donor and acceptor molecules at active sites for each inactive enzyme derivative that was treated with 46 μM $ZnCl_2$ in the presence of 9.2 mM $MgCl_2$ and 40 mM Hepes/KOH buffer, pH 7.0, at 25 °C. [b] R_0 values were assumed to be the same as those given in Table II. [c] Maximum percent quench values were observed 30–40 min after Zn^{2+} addition (see Figure 2). The values marked with an asterisk (*) were from two independent measurements in which the same value was obtained twice; other percent transfer values are from one measurement. [d] The observed maximum percent quench values were corrected approximately for unquenched ends of linear aggregates by adding 8 and 17% to observed values for stacking enzyme derivatives with 1 and 2 equiv of donors/dodecamer, respectively. [e] R is the calculated intermolecular distance between active site probes (donor to one acceptor) on face to face dodecamers in linear aggregates, using the corrected value for percent energy transfer for each enzyme derivative, the corresponding R_0 value, and the Förster equation (eq 1).

separately in Table III since increasing the number of donors in a dodecamer should increase the probability of two donors being placed opposite each other in stacked dodecamers, in which case energy transfer will not occur. In order to calculate approximate intermolecular distances between donor and acceptor probes on active sites of face to face dodecamers in linear aggregates, we have applied corrections to the observed transfer efficiencies for the presence of unquenched fluorescent probes at ends of linear aggregates 30–40 min after Zn^{2+} addition. The maximum quench in fluorescence appeared to occur when the average length of face to face aggregates corresponded to a 6-mer of stacked dodecamers (see above). The stacking of six dodecamers will result in one-sixth of the original hexagonal surface areas being exposed at the two ends of the face to face linear aggregate. With one fluorescent donor per dodecamer, the corresponding correction for unquenched ends of a 6-mer is $^1/_{12}$th or 8%. When enzyme derivatives contained an average of two fluorescent donors/dodecamer (on the same or on opposite hexagonal rings), the percent of unquenched ends in a 6-mer linear aggregate is one-sixth or 17% of the original fluorescence. Accordingly, corrections of 8 or 17% were added to each observed maximum percent quench value in Table III for enzyme derivatives containing one or two donors/dodecamer, respectively.

The intermolecular energy-transfer distances (R) calculated from eq 1 also are given in Table III. Calculated values of R for most of the enzyme derivatives agreed well and indicate that the average intermolecular distance between donor and acceptor nucleotide probes on active sites in face to face aggregates is ~36 Å. The distances between donor and acceptor probes on separate dodecamers in Zn^{2+}-induced stacks (~36 Å) are considerably shorter than those between probes within the same dodecamer (~56–60 Å). This result argues strongly that the active site probes are located toward exterior surfaces of hexagonal rings away from the lateral plane of the dodecamer in glutamine synthetase.

Discussion

ATP analogues (with bulky substituents at the 6- or 8-position of the purine ring) can be bound essentially irreversibly to active sites of glutamine synthetase in the presence of L-Met-(*S*)-sulfoximine and Mn^{2+} at pH 7 (Maurizi & Ginsburg, 1986). In addition, the fluorescence of 8-S-AEDANS-ATP or aza-ϵ-ATP bound to active sites was completely unaffected by binding ADP (or other ligands with poor spectral overlaps with the fluorescence emission) to other active sites of the dodecamer, indicating that protein conformational changes did not affect the fluorescence yield of the bound donor. This has greatly simplified the determination of energy transfer between donor and acceptor nucleotide analogues bound at different active sites within the dodecameric enzyme.

The intramolecular fluorescence energy transfer was determined by comparing the fluorescence yield of enzyme derivatives containing 1 or 2 equiv of fluorescent donor with other active sites occupied by either an acceptor (6-Y-ADP or 8-Y-ADP) or a nonacceptor (ADP). The same transfer efficiencies were measured for each donor/acceptor pair whether 1 or 2 equiv of the donor were bound per dodecamer, suggesting that fluorescent probes were not preferentially bound to adjacent subunits but were probably randomly distributed. We used low amounts of fluorescence donor and saturated the remaining sites with acceptor because the low efficiency of energy transfer would not have allowed accurate measurement of quenching if only a portion of sites adjacent to donor were occupied and also because we wanted to avoid the possibility of nonrandom distribution of acceptor analogues at less than saturating levels.

Several assumptions have been made in calculating the fluorescence energy transfer distances in Table II. For example, a value of $^2/_3$ was assigned for the orientation factor (κ^2 in eq 2), which is valid only for a random orientation between the emission dipole of the donor and the absorption dipole of the acceptor. Probes relatively free to rotate can often be assumed to have random orientations. However, fluorescence polarization measurements indicated that 8-S-AEDANS-ADP and aza-ϵ-ADP have rather restricted mobility when bound to the enzyme active site, and we assume that the Y-ADP analogues are equally restricted. The limiting polarization values for either enzyme-bound fluorescent probe (Table I) set lower and upper limits for κ^2 of ~0.07–3.5 (Dale et al., 1979), which is too large a range to be helpful since it gives calculated values of 22–50 Å for R_0. However, as discussed by others (Brand & Witholt, 1967; Stryer, 1978), the relative orientation of probes on different enzyme molecules may not be identical and, averaged over the entire population of enzyme–donor/acceptor complexes, the orientation between probes might be considered random. The probability of error in using an orientation factor of $^2/_3$ can be estimated by comparing distance measurements with different donors and acceptors since it is unlikely that different probes would adopt the same nonrandom orientations. We have used two fluorescent donors that are chemically and structurally different and two acceptors that are chemically the same but differ in their point of attachment to the nucleotide (and presumably orientation). The excellent agreement of the data for the four combinations of donors and acceptors would indicate that the average orientations of the probes are not greatly different

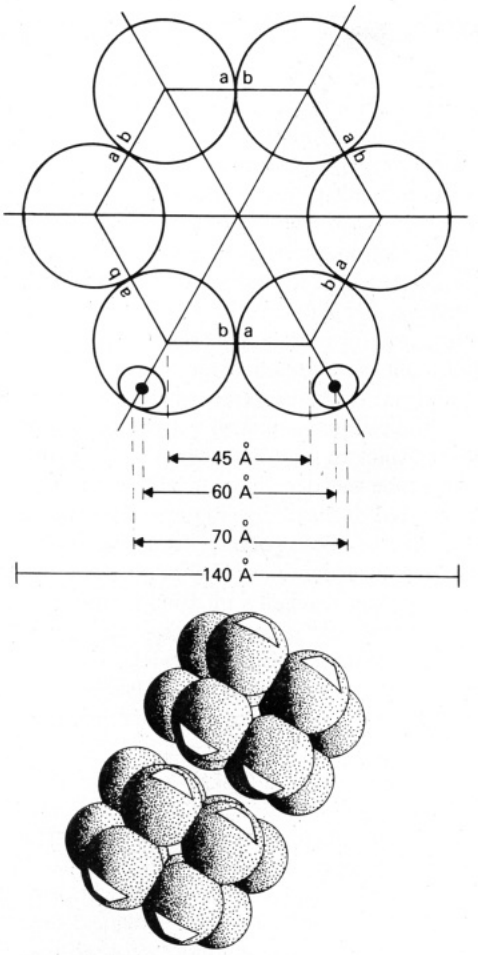

FIGURE 5: Molecular dimensions of *E. coli* glutamine synthetase. The geometry and distances between centers of subunits and the diameter of one of the two hexagonal rings of the molecule are based on the electron microscopic images of Valentine et al. (1968). The binding of the subunits to form a closed hexagonal ring is shown to depend on sites a and b, which participate in heterologous association. The enzyme has 6-fold dihedral symmetry with a second hexagon inverted on top of the first to form isologous contacts between rings. For illustrative purposes (see text), active sites are depicted as spheres approximately 12 Å in diameter located at the outer and upper edges of subunits within a hexagonal ring. Below, two molecules of glutamine synthetase as a face to face aggregate (viewed from a 45° angle) have been drawn with the aid of a computer-imaging program of Richard J. Feldmann (Molecular and Cellular Graphics, NIH). The distance between centers of subunits in the same dodecamer is ~45 Å, and that between centers of opposing subunits in stacked dodecamers is ~55 Å. The limits on probable locations of an active site probe on each subunit are indicated by the outlined white areas on the most visible subunits. These areas are approximated for surfaces 6 Å below exteriors. It can be seen that distances between probes at active sites within a hexagonal ring are potentially closer than those between probes in active sites in opposite rings.

from the random orientation and that there is minimal error in assuming a value of $^2/_3$ for κ^2. A second and perhaps a major factor contributing to the randomizing of the orientation is that our data are best interpreted in terms of energy transfer from a single donor to *two* equidistant acceptors with a minor component of transfer to a third possibly more distant acceptor within the same molecule (see below).

Probable Location of Active Sites in Dodecameric Glutamine Synthetase. Glutamine synthetase appears as a symmetrical dodecamer with two superimposed hexagonal rings in the electron microscopic images obtained by Valentine et al. (1968). The maximum distance across a hexagonal ring is ~140 Å and the distance between centers of adjacent subunits within the ring is ~45 Å (Figure 5). The distance between centers of superimposed subunits from opposite hexagonal rings is also ~45 Å. If one assumes that the subunits within a hexagonal ring are heterologously bonded as proposed by Valentine et al. (1968), the distance between identical points at the outer edge of the ring is 70 Å (Figure 5). However, the active site of a subunit of the enzyme must accommodate three substrates, two divalent cation sites, and a nearby adenylylation site. Measurements of distances between active site ligands from several laboratories indicate that the minimum volume occupied by the active site of each subunit can be approximated by a sphere of ~12 Å in diameter (Villafranca et al., 1978). A reasonable estimate of the position of a probe at the active site would be ~6 Å below the surface; and thus, the maximum distance between probes located at the centers of active sites on adjacent subunits within a hexagonal ring is close to 60 Å (Figure 5).[3] Assuming isologous contacts between opposing subunits from the two hexagonal rings, the maximum distance between centers of active sites on these subunits is ~78 Å if active sites are located on the exterior surfaces away from the lateral plane between rings.

Initially, we calculated R assuming one donor and one acceptor. This calculated distance is a *minimum* distance between sites. If transfer occurs to more than one acceptor, the efficiency of transfer to any one site is less than the total, and the calculated distance to that site will be greater. The apparent efficiency of transfer was ~24% for 8-S-AEDANS-ADP and ~34% for aza-ϵ-ADP, and the corresponding distance (R) was ~49 Å. The low efficiency of energy-transfer and the rather large minimum distance between probes (≥49 Å) essentially rule out close contact between any two sites. Since the active sites appear somewhat distant from each other, the observed energy transfer must occur between the donor and more than one acceptor.

By use of the Förster equation, the calculated values of R_0 (Table II), and the maximum distance between active sites in a hexagonal ring (60 Å), the minimum efficiency of energy transfer between donor and acceptor bound to adjacent subunits in the same hexagonal ring is calculated to be 9% for 8-S-AEDANS-ADP and 11% for aza-ϵ-ADP. Since there are two equidistant active sites in the same ring, the minimum transfer is 17% for 8-S-AEDANS-ADP and 21% for aza-ϵ-ADP when all remaining active sites are occupied by acceptor. The minimum values are not greatly different from the observed percent quench values, and therefore, most of the observed energy transfer must occur between active sites within hexagonal rings. The additional energy transfer over the calculated minimum possibly could result from the active sites being slightly closer together (~56 Å) with no significant transfer to any other site or from transfer to yet another site. Thus, the data are consistent with transfer to *three* equidistant acceptor sites as would be the case if active site probes on isologously bonded subunits as well as those on heterologously bonded subunits are 60 Å apart.

The location of active site probes toward exterior surfaces of hexagonal rings of the dodecamer was confirmed by fluorescence energy transfer measurements in face to face linear aggregates (formed along the 6-fold axes of dodecamers) of the same enzyme derivatives. With 8-S-AEDANS-ADP or ϵ-aza-ADP on a dodecamer subunit opposite a subunit from another molecule containing 8-Y-ADP or 6-Y-ADP acceptor, 47–70% quench of fluorescence was observed. After corrections for unquenched polymer ends, the efficiency of energy transfer assuming transfer from donor to a single acceptor indicated that there is ~36 Å between active site probes on

face to face dodecamers. If active sites are not vertically aligned in stacks, transfer to more than one acceptor on different subunits of the opposing dodecamer is possible. Calculations assuming transfer to two equidistant acceptors gave a distance of ~42 Å to each acceptor. Given these distances and by using 60 Å as the distance between adjacent active sites in the same ring, the separation of planes defined by the active site probes was determined by triangulation to be ~29 Å. In fact, 36 Å, the distance between vertically aligned active site probes, is the maximum intermolecular distance between active site planes, and the actual distance is 29–36 Å.

Electron microscopic images show that each space between face to face dodecamers in linear aggregates is greater than that between hexagonal rings in the same molecule (Valentine et al., 1968; Miller et al, 1974; Frey et al., 1975; Frey & Eisenberg, 1984; Lipka et al., 1984). The distance between centers of superimposed subunits in two dodecamers is ~55 Å and the total thickness of the dodecamer in a stack is ~100 Å. The distance of ~36 Å measured between active sites on layered dodecamers agrees well with that expected if active sites on isologously bonded subunits are 60 Å apart (100 Å − 60 Å = 40 Å). The estimate of an approximate 36-Å separation of active site probes on facing dodecamers represents an average value if there is flexibility in intermolecular bonding domains in face to face linear aggregates, as suggested by the data of Frey & Eisenberg (1984). In the case of active sites being maximally displaced from a vertical alignment, the distance between the lateral planes defined by active sites in hexagonal rings of opposing dodecamers is still ≤40 Å. Thus, the data clearly indicate that the distance between active sites in opposing rings of stacked dodecamers is considerably shorter (≤40 Å) than that between active sites in opposite rings of the same dodecamer (≥60 Å).

We can conclude definitely that the active sites are near the exterior surfaces away from the central 6-fold axis of the dodecamer.[3] The set of chemically identical points 55–60 Å apart on heterologously bonded subunits is described in the upper drawing of Figure 5 by a curved surface cutting the subunits near the outer surface and normal to the lateral plane of the dodecamer. We also know that no two active sites on isologously bonded subunits can be closer than ~61 Å so that active sites must be away from the lateral plane of the dodecamer and beyond the centers of the subunits, which are only 45 Å apart. The open (white) sections on the lower drawing in Figure 5 show our estimates for the limits of the probable locations of active site probes for the two cases of either *two* acceptors (isologous active sites distant) or *three* acceptors (isologous and heterologous active sites equidistant). The sizes of these outlined white areas approximate those expected for the surfaces 6 Å below exterior surfaces. Our results are consistent with the results of Frink et al. (1978), who located the sites of adenylylation on the outer edges of the glutamine synthetase molecule, since the adenylylation site should be no more than 12 Å from the nucleotide probe at the active site.

The observations of Frey & Eisenberg (1984) on Co^{2+}-induced face to face aggregation of glutamine synthetase suggest that there is some twisting of single strands along the 6-fold axial symmetry. As discussed by these investigators, protein–protein interactions of the types described by Chothia & Janin (1975) could be conserved in stacking and still result in the movement of one surface relative to another if each enzyme subunit has two or more domains connected by a flexible hinge. Such flexibility in intermolecular bond formation allows for a lower entropy decrease in self-assembly than would be formally calculated for the loss of translational and rotational freedom (Steinberg & Scheraga, 1963; Erickson, 1979). Certainly, Co^{2+}- or Zn^{2+}-induced face to face aggregation of the enzyme occurs spontaneously as do biologically important protein self-assemblies.

An Arrhenius activation energy of 22.3 ± 0.2 kcal/mol was measured here for Zn^{2+}-induced stacking of dodecamers in the presence of 9 mM $MgCl_2$ at pH 7.0. This is a rather low activation energy considering that Zn^{2+} binding promotes a conformational change in each protein subunit (Miller et al., 1974; Ginsberg, 1972) and that the stacking reaction involves the simultaneous formation of six identical contacts between pairs of subunits in two dodecamers.

Intermolecular fluorescence energy transfer measurements also have allowed preliminary studies of the kinetics of Zn^{2+}-induced stacking of dodecamers, since the quench of the fluorescent probe was dependent on the presence of acceptor probes in layered dodecamers (Figure 2) and correlated well with the degree of linear polymer formation (Figures 3 and 4B). The time-dependent fluorescence quench during the face to face aggregation reached a maximum value when the average *n*-mer was six dodecamers, after which time side to side aggregation predominates over polymer elongation. The second-order rate plots of Figure 4C were based on fluorescence changes and provide strong support for energy transfer occurring as a result of a bimolecular process. From fluorescence changes, the initial stages of the Zn^{2+}-induced face to face aggregation with either AEDANS-ADP or aza-ϵ-ADP as the protein-bound fluorescent probe were determined to have a second-order rate constant of $\sim 10^5\ s^{-1}\ M^{-1}$ at pH 7.0 and 25 °C, where M is the molar concentration of dodecamer. The Zn^{2+}-induced stacking of enzyme dodecamers and the quench of enzyme-bound fluorescent probes could be rapidly and completely reversed by the addition of EDTA. This indicates that the association constant for Zn^{2+} in linear aggregates is $\leq 10^{14}\ M^{-1}$ and that the kinetics of depolymerization could be monitored by fast reaction techniques. Some of the approaches used here should be generally applicable to kinetic studies of self-assembly reactions of other proteins when donor and acceptor probes are attached.

Conclusions

We began this study to determine whether the kinetic and binding data that indicated some form of communication between active sites of glutamine synthetase could be explained by the proximity of pairs of active sites in the dodecamer. The stabilization of submolecular oligomers by active site ligands implies that ligands binding at the active site alter the structure of the intersubunit bonding domains. These conformational changes may also extend to adjacent active sites leading to enhanced binding of inactivating ligands and thus to a nonrandom distribution of inactive subunits in partially inactivated dodecamers. However, our results show that no two active sites of glutamine synthetase are closer to each other than to active sites on other adjacent subunits. Rather, it appears that the active site nucleotide probes are arranged symmetrically within 4 Å of being at the maximum distance apart and that nucleotides at active sites of the heterologously bonded subunits are equidistant (~56–60 Å) from each other. Active site probes of the subunits in the opposite ring are ≥60 Å apart and located on the outer surface of the dodecamer away from the central 6-fold axis of symmetry. The location of the active sites with respect to the subunit bonding domains is under investigation, but our results suggest that the nucleotide probes are near (±5 Å) a longitudinal plane equidistant from the subunit contacts.

ACKNOWLEDGMENTS

We are grateful to Dr. James J. Lipka and other staff members under the direction of Drs. Joseph S. Wall and James F. Hainfeld for electron microscopic (STEM) analysis of our samples at the Brookhaven National Laboratory (supported by NIH Grant RR01777 and the U.S. DOE). We also thank Dr. Richard J. Feldmann in Molecular and Cellular Graphics at NIH for his computer imaging of two stacked dodecamers.

Registry No. GS, 9023-70-5; 8-S-AEDANS-ATP, 99376-89-3; aza-ε-ATP, 50663-89-3; 8-Y-ATP, 99376-91-7; 6-Y-ATP, 99376-90-6; 8-mercapto-ATP, 41106-66-5; iodo-Y, 77145-08-5; 6-mercaptopurine ribonucleoside triphosphate, 27652-34-2.

REFERENCES

Azumi, T., & McGlynn, S. P. (1962) *J. Chem. Phys. 37*, 2413–2420.

Bild, G. S., & Boyer, P. D. (1980) *Biochemistry 19*, 5774–5781.

Brand, L., & Witholt, B. (1967) *Methods Enzymol. 11*, 776–856.

Chen, R. F. (1967) *Anal. Biochem. 20*, 339–357.

Chothia, C., & Janin, J. (1975) *Nature (London) 256*, 705–708.

Dale, R. E., Eisinger, J., & Blumberg, W. E. (1979) *Biophys. J. 26*, 161–193.

Denton, M. D., & Ginsburg, A. (1970) *Biochemistry 9*, 617–632.

Erickson, H. P. (1979) *Biophys. J. 25*, 233a.

Förster, T. (1959) *Discuss. Faraday Soc. 27*, 7–17.

Frey, T. G., & Eisenberg, D. (1984) *Int. J. Biol. Macromol. 6*, 2–12.

Frey, T. G., Eisenberg, D., & Eiserling, F. A. (1975) *Proc. Natl. Acad. Sci. U.S.A. 72*, 3402–3406.

Frink, R. J., Eisenberg, D., & Glitz, D. G. (1978) *Proc. Natl. Acad. Sci. U.S.A. 75*, 5778–5782.

Ginsburg, A. (1972) *Adv. Protein Chem. 26*, 1–79.

Haschemeyer, R. H., Wall, J. S., Hainfeld, J. F., & Maurizi, M. R. (1982) *J. Biol. Chem. 257*, 7252–7253.

Hudson, E. N., & Weber, G. (1973) *Biochemistry 12*, 4154–4161.

Hunt, J. B., & Ginsburg, A. (1972) *Biochemistry 11*, 3723–3735.

Hunt, J. B., & Ginsburg, A. (1980) *J. Biol. Chem. 255*, 590–594.

Hunt, J. B., Smyrniotis, P. Z., Ginsburg, A., & Stadtman, E. R. (1975) *Arch. Biochem. Biophys. 166*, 102–124.

Lipka, J. J., Hainfeld, J. F., & Wall, J. S. (1984) *Proceedings of the 42nd Annual Meeting of the Electron Microscopy Society of American* (Bailey, G. W., Ed.) pp 158–159, San Francisco Press, San Francisco.

Luedtke, R., Owen, C. S., Vanderkooi, J. M., & Karush, F. (1981) *Biochemistry 20*, 2927–2936.

Maurizi, M. R., & Ginsburg, A. (1982a) *J. Biol. Chem. 257*, 4271–4278.

Maurizi, M. R., & Ginsburg, A. (1982b) *J. Biol. Chem. 257*, 7246–7251.

Maurizi, M. R., & Ginsburg, A. (1985) *Curr. Top. Cell. Regul. 26*, 191–206.

Maurizi, M. R., & Ginsburg, A. (1986) *Biochemistry* (preceding paper in this issue).

Meister, A. (1974) *Enzymes (3rd Ed.) 10*, 699–754.

Miller, R. E., Shelton, E., & Stadtman, E. R. (1974) *Arch. Biochem. Biophys. 163*, 155–171.

Mosesson, M. W., Hainfeld, J. F., Haschemeyer, R. H., & Wall, J. S. (1981) *J. Mol. Biol. 153*, 695–718.

Parker, C. A., & Rees, W. T. (1966) *Analyst (London) 85*, 587–600.

Rhee, S. G., Chock, P. B., Wedler, F. C., & Sugiyama, Y. (1981) *J. Biol. Chem. 256*, 644–648.

Scott, T. G., Spencer, R. D., Leonard, N. J., & Weber, G. (1970) *J. Am. Chem. Soc. 92*, 687–695.

Shapiro, B. M., & Ginsburg, A. (1968) *Biochemistry 7*, 2153–2167.

Shrake, A., Powers, D. M., & Ginsburg, A. (1977) *Biochemistry 16*, 4372–4381.

Shrake, A., Ginsburg, A., Wedler, F. C., & Sugiyama, Y. (1982) *J. Biol. Chem. 257*, 8238–8243.

Stadtman, E. R., & Ginsburg, A. (1974) *Enzymes (3rd Ed.) 10*, 755–807.

Stadtman, E. R., Smyrniotis, P. Z., Davis, J. N., & Wittenberger, M. E. (1979) *Anal. Biochem. 95*, 275–285.

Steinberg, I. Z., & Scheraga, H. A. (1963) *J. Biol. Chem. 238*, 172–181.

Stryer, L. (1978) *Annu. Rev. Biochem. 47*, 819–846.

Valentine, R. C., Shapiro, B. M., & Stadtman, E. R. (1968) *Biochemistry 7*, 2143–2152.

Villafranca, J. J., Rhee, S. G., & Chock, P. B. (1978) *Proc. Natl. Acad. Sci. U.S.A. 75*, 1255–1259.

Wedler, F. C., Sugiyama, Y., & Fisher, K. E. (1982) *Biochemistry 21*, 2168–2177.

Yip, K. F., & Tsou, K. C. (1973) *Tetrahedron Lett. 33*, 3087–3090.